Progress In Electromagnetics Research C, Vol. 130, 43–55, 2023

Ultra Compact Flexible Monopole Antennas for Tri-Band Applications

Reshma Lakshmanan[1, *], Shanta Mridula[1], Anju Pradeep[1], and Kinatingal Neema[2]

Abstract—Two novel ultra-compact flexible tri-band antennas with coplanar waveguide (CPW) feed and asymmetric coplanar strip (ACS) feed arrangements are presented in this paper. These antennas are fabricated on an extremely thin substrate with dielectric constant (ε_r) 3.5 and loss tangent ($\tan\delta$) 0.027. The folded geometry of the antennas contributes to the size reduction. While the CPW-fed tri-band antenna (19 mm × 19 mm) exhibits bandwidth of 130 MHz, 600 MHz, and 1550 MHz in the lower, middle, and upper frequency bands, the ACS-fed tri-band antenna (19.5 mm × 15 mm) exhibits 80 MHz, 600 MHz, and 2220 MHz bandwidth, respectively. Design equations are developed, and an appropriate circuit model is recommended. The performance of the antenna is investigated for various bending conditions. Simple geometry, compactness, flexibility, and stability under bending conditions over multiband make these incredibly thin antennas quite appealing for ISM 2.4/5.2 GHz, Wi-Fi 2.4/5 GHz, WLAN 2.4/5.2/5.8 GHz and WiMAX 3.5/5.5 GHz applications.

1. INTRODUCTION

Versatility and miniaturization are the key features of emerging electronic gadgets in the present world. Multiband antennas on flexible substrates are popular for such applications. Among multiband antennas, tri-band antennas are well known [1–9]. Tri-band antennas are designed to operate in three different frequency bands. The popular bands for these applications are DCS 1.89 GHz, LTE (1.96–2.22 GHz), 5G mid band (2.35–2.5 GHz/3.18–3.82 GHz/4.15–5.42 GHz), ISM (2.4–2.48 GHz/5.2–6 GHz), WLAN (2.4–2.484 GHz/5.15–5.35 GHz/5.725–5.825 GHz), and WiMAX (3.4–3.6 GHz/5.28–5.85 GHz) [4–8].

Compactness and flexibility are important attributes of antennas. The compactness of an antenna is mainly achieved by the proper selection of antenna geometry. A flexible substrate leads to the flexibility of any antenna. Different flexible materials for numerous applications have been reported, Rogers R04835T [1], polyamide [2], polyimide [3], Dupont [10, 11], kapton polyimide [12], polyethylene terephthalate (PET) [13], RT-5880 [14] to name a few. Octagonal patch [1], slotted patch [2, 9], tri-annular square ring [3], triangular monopole [4], and fractal geometry [5] are the different multiband antennas proposed on flexible substrates. Microstrip, coplanar waveguide (CPW) coaxial, aperture coupled, proximity coupled, and asymmetric coplanar strip (ACS) are the various feeding techniques employed for these antennas. The authors have reported compact CPW and ACS fed dual band antennas on flexible Dupont substrates [10, 11].

This paper presents two novel ultra-compact flexible tri-band antennas with CPW feed and ACS feed designed on extremely thin flexible substrates. Folded geometry is used in this work to reduce the overall antenna size. Easy fabrication process is one of the attractive features of the proposed antennas. Compactness and flexibility of the antennas make them suitable where bending situations

Received 9 November 2022, Accepted 7 February 2023, Scheduled 20 February 2023
* Corresponding author: Reshma Lakshmanan (lakshmananreshma@gmail.com).
[1] Division of Electronics Engineering, School of Engineering, Cochin University of Science and Technology, Cochin, Kerala, India.
[2] Department of Electronics, Cochin University of Science and Technology, Cochin, Kerala, India.

are encountered. Therefore, detailed bending investigations are conducted. The proposed antennas are simulated, fabricated, and tested under experimental conditions to validate their performance.

2. ANTENNA STRUCTURE AND DESIGN

The design of compact coplanar waveguide (CPW) and asymmetric coplanar strip (ACS) fed tri-band flexible monopole antennas (TBFMAs) is explained in this section.

2.1. Compact CPW-Fed Tri-Band Flexible Monopole Antenna (TBFMA)

The proposed compact coplanar waveguide (CPW) fed tri-band flexible monopole antenna (TBFMA) comprises three resonant sections catering to the different application bands. Figs. 1(a)–(d) show the development phases of the proposed CPW-fed TBFMA. The corresponding reflection coefficient plot (S_{11} in dB) is shown in Fig. 1(e). The 19 mm × 19 mm antenna is designed on an extremely thin Dupont substrate with height (h) 130 µm, dielectric constant (ε_r)3.5, and loss tangent ($\tan\delta$)0.027. The simulations are done using Computer Simulation Technology (CST) software. Size miniaturization of monopole antennas at low frequencies is the main motivation of the proposed design. This is accomplished by folding a straight monopole to create a meandered antenna (P-1) formed by strip d_s and folded strips $d_2 + d_3 + d_4 + d_5 + d_6$, as shown in Fig. 1(a), obtaining a resonance at 2.72 GHz in the lower resonant band. In order to achieve the upper resonance in the 5.5 GHz application band, the strip d_1 is attached to P-1, resulting in an inverted L formed by d_s and d_1. As a result, an additional resonance at 5.75 GHz is achieved; the developed antenna (P-2) is presented in Fig. 1(b). The strips $d_7 + d_8 + d_9$ added to P-2, resulting in a C-shaped structure formed by d_m and $d_7 + d_8 + d_9$, produce a resonance in the middle band at 3.62 GHz. The modified geometry (P-3) is shown in Fig. 1(c). The narrow slit introduced in P-3 results in the final geometry (P-4), as shown in Fig. 1(d). This helps to tune out the unwanted resonance. In the course of evolution, a lower shift in resonances is observed as

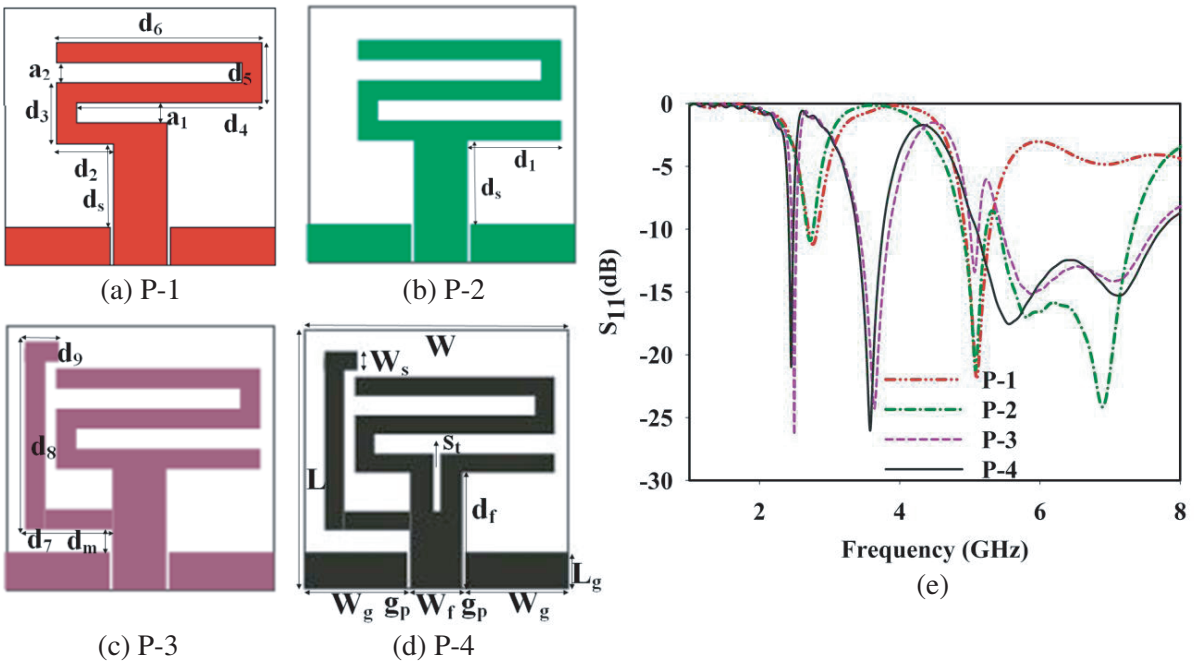

Figure 1. (a)–(d) Development phases of the proposed CPW fed TBFMA (ε_r = 3.5, h = 130 µm, W = 19 mm, L = 19 mm, d_s = 6.2 mm, d_m = 1.7 mm, L_g = 2.8 mm, W_g = 7.8 mm, d_f = 9 mm, W_f = 4 mm, W_s = 1.5 mm, d_1 = 7 mm, d_2 = 4.2 mm, d_3 = 4.5 mm, d_4 = 13.7 mm, d_5 = 4.5 mm, d_6 = 15.2 mm, d_7 = 6.5 mm, d_8 = 14 mm, d_9 = 2.5 mm, g_p = 0.2 mm, s_t = 0.3 mm, a_1 = 1.5 mm, a_2 = 1.5 mm). (e) Reflection coefficient (dB) plot of antennas in the development phases.

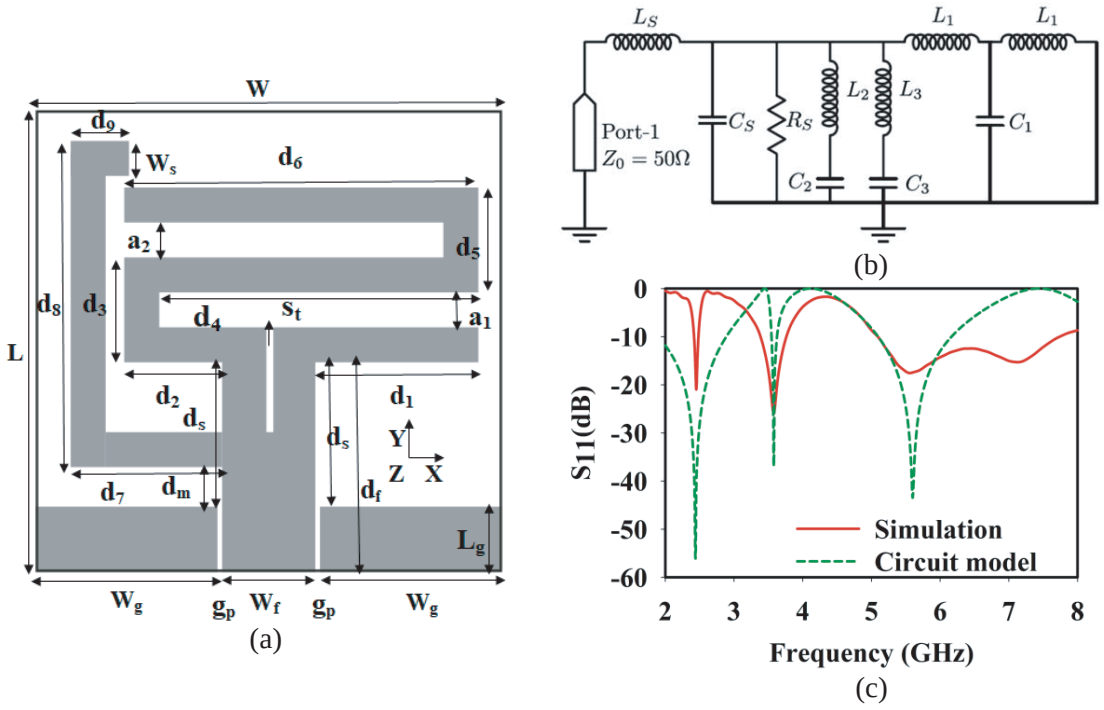

Figure 2. (a) CPW fed TBFMA geometry. (b) Circuit model of the antenna developed using ADS. (c) Corresponding reflection coefficient plot.

strips are subsequently added to the folded antenna (P-1). The dimensions of the strips are optimized to obtain the resonances in the required bands. The developed antenna (Fig. 2(a)) operates in three frequency bands 2.4 to 2.48 GHz (80 MHz), 3.37–3.77 GHz (400 MHz), and 5.1– to 7.7 GHz (2600 MHz), resonating at 2.45 GHz, 3.57 GHz, and 5.59 GHz, respectively. The design equations are developed from parametric analysis as detailed below.

Figure 2(b) illustrates the circuit model for the proposed CPW-fed TBFMA. The 50 Ω CPW feed, folded monopole, inverted L-shaped and C-shaped structure contributing to various resonances are modelled in the proposed circuit. The elements R_S (50 Ω), L_S (0.165 nH), and C_S (0.5 pF) represent the CPW feed. The T-shaped circuit elements L_1 (1.5 nH) and C_1 (0.61 pF), denoting the folded strip ($d_S+d_2+d_3+d_4+d_5+d_6 = 0.58\lambda$), provide the lower resonance at 2.44 GHz (f_1); the circuit elements C_2 (0.115 pF) and L_2 (18.5 nH), denoting the C-shaped open stub ($d_m+d_7+d_8+d_9 = 0.28\lambda$), contribute to the middle resonance at 3.58 GHz (f_2); and the circuit elements L_3 (3.93 nH) and C_3 (0.38 pF), denoting the inverted L-shaped open stub ($d_S+d_1 = 0.242\lambda$), contribute to the upper resonance at 5.6 GHz (f_3). Fig. 2(c) shows the reflection coefficient plot (S_{11} in dB) of the circuit simulated using Advanced Design System (ADS) software. The plot clearly indicates the three resonant bands.

The impact of antenna dimensions on different antenna characteristics has been studied by parametric analysis. It is found that the ground dimensions (L_g and W_g) mainly affect the impedance. To achieve the intended performance, $L_g \times W_g$ of the proposed CPW-fed TBFMA is optimized to 2.8 mm × 7.8 mm. The design equations are:

$$d_{t1} = -5.685f_1 - 0.126\varepsilon_r - 8.32h + 63; \quad (1)$$

$$\text{where} \quad d_{t1} = d_S + d_2 + d_3 + d_4 + d_5 + d_6$$

$$d_{t2} = -5.93f_2 - 0.2\varepsilon_r - 11.708h + 48.2; \quad (2)$$

$$\text{where} \quad d_{t2} = d_m + d_7 + d_8 + d_9$$

$$d_{t3} = -3.18f_3 - 0.19\varepsilon_r - 9.31h + 32.9; \quad (3)$$

$$\text{where} \quad d_{t3} = d_S + d_1$$

h is the height of substrate in mm, and ε_r is the dielectric constant of the material. The lengths of the

individual strips of the folded monopole which make up d_{t1} are limited by the dimensions of the gaps a_1, a_2 defined by the following equations.

$$a_1 = -3.08h - 0.056\varepsilon_r - 2.334f_1 + 7.84 \quad (4)$$

$$a_2 = -4.15h - 0.069\varepsilon_r - 2.628f_1 + 8.72 \quad (5)$$

Equations (1)–(5) are valid for $h \leq 0.2$ mm and $2.2 \leq \varepsilon_r \leq 4.4$. The resonant length is calculated for various substrate heights (h), dielectric constant (ε_r), and frequencies to validate the above equations. Table 1 shows the % error in resonant length of the proposed CPW-fed TBFMA. The observed error is less than 2%.

Table 1. Error in resonant length of proposed CPW fed TBFMA.

Substrate		Frequencies (GHz)			Resonant length (mm)						Error (%)		
					Equation			Simulation					
ε_r	h (mm)	f_1	f_2	f_3	d_{t1}	d_{t2}	d_{t3}	d_{t1}	d_{t2}	d_{t3}	d_{t1}	d_{t2}	d_{t3}
4.4	0.025	2.6	3.6	5.5	47.36	25.4	14.3	48.3	25.7	14.2	1.9	1.2	0.7
2.2	0.05	2.7	3.7	6.3	46.86	25.2	12	47.3	24.7	12.2	0.93	1.9	1.63
Proposed CPW fed TBFMA													
3.5	**0.13**	**2.45**	**3.57**	**5.59**	**47.54**	**24.8**	**13.3**	**48.3**	**24.7**	**13.2**	**1.57**	**0.4**	**0.05**

2.2. Compact ACS Fed Tri-Band Flexible Monopole Antenna (TBFMA)

Asymmetric coplanar strip (ACS) feeding is another technique used in compact planar antenna design. The asymmetrical nature of the structure contributes to size miniaturization. Figs. 3(a)–(c) show the development phases of the proposed ACS-fed TBFMA. The corresponding reflection coefficient plot is

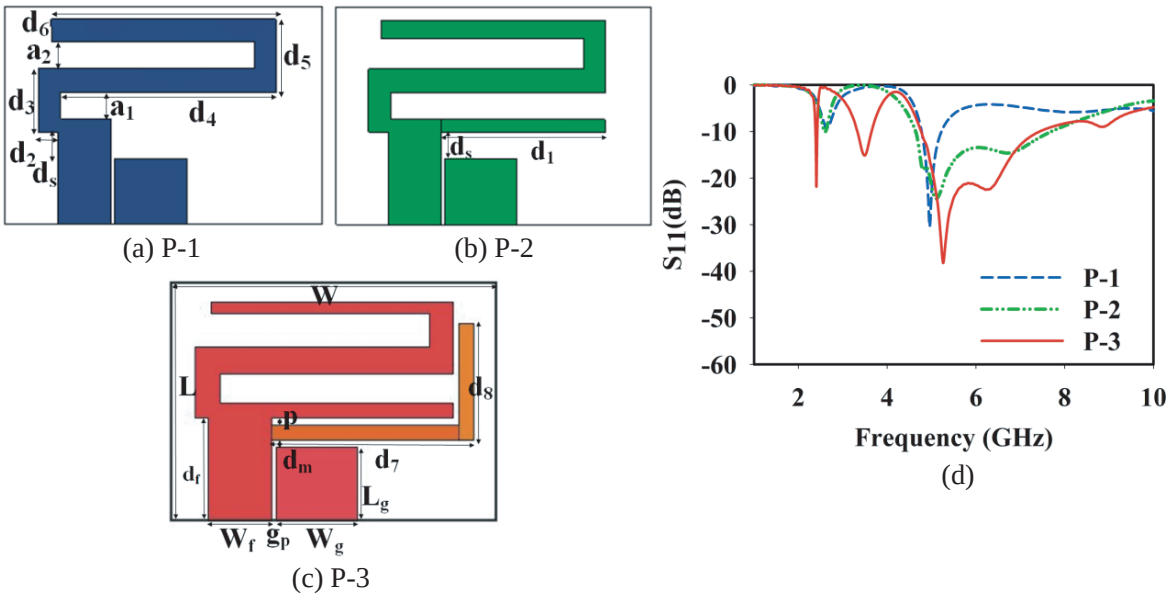

Figure 3. (a)–(c) Development phases of the proposed ACS-fed TBFMA ($\varepsilon r = 3.5$, $h = 50\,\mu$m, $W = 19.5$ mm, $L = 15$ mm, $d_s = 2$ mm, $L_g = 5$ mm, $W_g = 5.5$ mm, $d_f = 7$ mm, $W_f = 4$ mm, $d_1 = 12.5$ mm, $d_2 = 1.3$ mm, $d_3 = 4.8$ mm, $d_4 = 16.3$ mm, $d_5 = 4.85$ mm, $d_6 = 17$ mm, $d_7 = 13.9$ mm, $d_8 = 8.7$ mm, $g_p = 0.3$ mm, $d_m = 0.5$ mm, $p = 0.5$ mm, $a_1 = 2$ mm, $a_2 = 2.3$ mm). (d) reflection coefficient plot (dB) plot of antennas in the development phases.

shown in Fig. 3(d). The 19.5 mm × 15 mm antenna is designed on an extremely thin Dupont substrate with height (h) 50 µm, dielectric constant (ε_r) of 3.5, and loss tangent ($\tan\delta$) of 0.027. To miniaturize the monopole antennas, the straight monopole is folded to create a meandered geometry (P-1) formed by strip d_s and folded strips $d_2 + d_3 + d_4 + d_5 + d_6$, as presented in Fig. 3(a), and a resonance is obtained at 2.64 GHz in the lower resonant band. In order to achieve the upper resonance in the 5 GHz application band, strip d_1 is attached to P-1, resulting in an inverted L formed by d_s and d_1. Thus an additional resonance at 5.26 GHz is achieved, and the modified structure (P-2) is shown in Fig. 3(b). The strips $d_7 + d_8$ added to P-2, resulting in a L-shaped structure formed by d_m and $d_7 + d_8$, produce an additional resonance in the middle band at 3.5 GHz. The final geometry (p-3) is shown in Fig. 3(c). In the course of evolution, a shift in resonances is observed as strips are subsequently added to the folded antenna (P-1). The dimensions of the strips are optimized to obtain the resonances in the required bands. The asymmetric ground and folded geometry are responsible for the compactness. The developed antenna (Fig. 4(a)) operates in three frequency bands 2.38–2.43 GHz (50 MHz), 3.3–3.65 GHz (350 MHz), and 4.76–7.4 GHz (2640 MHz), resonating at 2.4 GHz, 3.5 GHz, and 5.3 GHz, respectively. The design equations are developed from parametric analysis as detailed below.

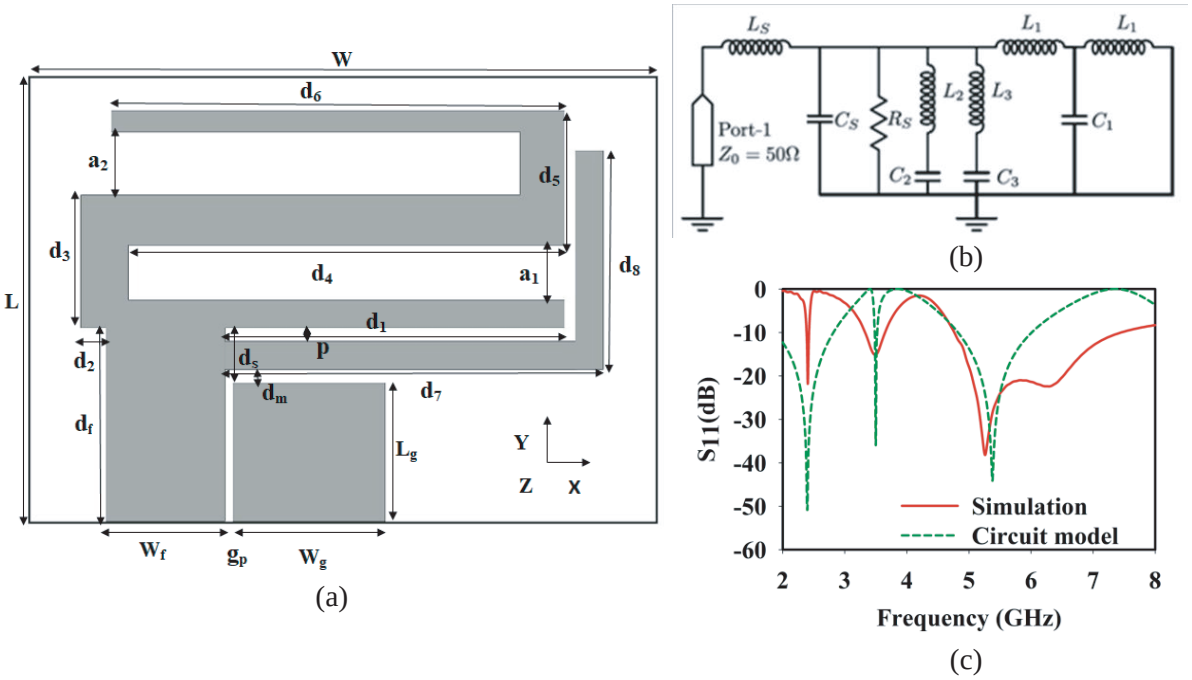

Figure 4. (a) ACS-fed TBFMA geometry. (b) Circuit model of the proposed antenna developed using ADS. (c) Corresponding reflection coefficient plot.

Figure 4(b) depicts the circuit model for the proposed ACS-fed TBFMA. The 50 Ω ACS feed, folded monopole, L-shaped and inverted L-shaped structure contributing to various resonances are modelled in the proposed circuit. The elements R_S (50 Ω), L_S (0.165 nH), and C_S (0.5 pF) represent the ACS feed. The T-shaped circuit elements L_1 (1.51 nH) and C_1 (0.62 pF), denoting the folded strip ($d_S + d_2 + d_3 + d_4 + d_5 + d_6 = 0.55\lambda$), provide the lower resonance at 2.4 GHz (f_1); the circuit elements C_2 (0.118 pF) and L_2 (18.5 nH), denoting the L-shaped open stub ($d_m + d_7 + d_8 = 0.269\lambda$), provide middle resonance at 3.5 GHz (f_2); and the circuit elements L_3 (4.5 nH) and C_3 (0.38 pF), denoting the inverted L-shaped open stub ($d_S + d_1 = 0.28\lambda$), contribute to the upper resonance at 5.38 GHz (f_3). Fig. 4(c) displays the reflection coefficient plot (S_{11} in dB) of the circuit simulated using ADS software. The plot clearly indicates the three resonant bands.

The impact of antenna dimensions on the different antenna characteristics has been studied by parametric analysis. To achieve the intended performance, L_g and W_g of the proposed ACS-fed TBFMA

are optimized to 5.5 mm and 5 mm. The design equations are:

$$d_{t1} = -12.5f_1 - 0.496\varepsilon_r - 27.15h + 79.6; \quad (6)$$
$$\text{where} \quad d_{t1} = d_S + d_2 + d_3 + d_4 + d_5 + d_6$$
$$d_{t2} = -9.34f_2 - 0.43\varepsilon_r - 19.43h + 58.3; \quad (7)$$
$$\text{where} \quad d_{t2} = d_m + d_7 + d_8$$

$$d_{t3} = -1.062f_3 - 0.027\varepsilon_r - 1.107h + 20.29; \quad (8)$$
$$\text{where} \quad d_{t3} = d_S + d_1$$

h is the height of substrate in mm, and ε_r is the dielectric constant of the substrate material. The lengths of the individual strips of the folded monopole which make up d_{t1} are limited by the dimensions of the gaps a_1, a_2 defined by the following equations.

$$a_1 = -5.6h - 0.111\varepsilon_r - 2.787f_1 + 9.384 \quad (9)$$
$$a_2 = -4.037h - 0.08\varepsilon_r - 2.04f_1 + 7.676 \quad (10)$$

Equations (6)–(10) are valid for $h \leq 0.2$ mm and $2.2 \leq \varepsilon_r \leq 4.4$. The resonant length is calculated for various substrate heights (h), dielectric constant (ε_r), and frequencies to validate the above equations. The % error in resonant length of the ACS-fed TBFMA is presented in Table 2. The observed error is less than 2%.

Table 2. % Error in resonant length of ACS-fed TBFMA.

Substrate		**Frequencies (GHz)**			**Resonant length (mm)**						**Error (%)**		
					Equation			**Simulation**					
ε_r	h (mm)	f_1	f_2	f_3	d_{t1}	d_{t2}	d_{t3}	d_{t1}	d_{t2}	d_{t3}	d_{t1}	d_{t2}	d_{t3}
4.4	0.025	2.49	3.6	5.25	45.67	21.83	14.56	45.25	22.1	14.6	0.9	1.22	0.27
2.2	0.13	2.37	3.54	5.4	45.35	21.76	14.39	45.25	22.1	14.4	0.22	1.53	0.69
Proposed ACS fed TBFMA													
3.5	**0.05**	**2.4**	**3.5**	**5.3**	**46.6**	**23.15**	**14.52**	**46.25**	**23.1**	**14.5**	**0.75**	**0.22**	**0.14**

3. RESULTS AND DISCUSSION

The parameters described in the previous section are used to build the antennas on a flexible DuPont substrate. Fabricated prototypes of the CPW-fed and ACS-fed TBFMAs are shown in Figs. 5(a) and 5(c). Experiments were done using Antritzu MS46122B Vector Network Analyzer (VNA). Figs. 5(b) and 5(d) show the reflection coefficient plots of the proposed CPW- and ACS-fed TBFMAs. The measured bandwidth of the CPW-fed TBFMA is 130 MHz (2.35 to 2.48 GHz) in the lower band, 600 MHz (3.1 to 3.7 GHz) in the middle band, and 1550 MHz (5.5 to 7.05 GHz) in the upper band. The measured bandwidth of the ACS-fed TBFMA is 80 MHz (2.39 to 2.47 GHz) in the lower band, 600 MHz (3 to 3.6 GHz) in the middle band, and 2220 MHz (4.78 to 7 GHz) in the upper band. These results reasonably agree with the simulated results presented in Figs. 1(e) and 3(d). ISM (2.4–2.48 GHz/5.2–6 GHz), WLAN (2.4–2.484 GHz/5.15–5.35 GHz/5.725–5.825 GHz) and WiMAX (3.4–3.6 GHz/5.28–5.85 GHz) communication bands are covered by the lower, middle, and upper bands.

Figures 6(a)–(c) show the surface current plots of CPW-fed TBFMA at 2.45 GHz, 3.5 GHz, and 5.5 GHz. The resonance at 2.45 GHz shown in Fig. 6(a) is mainly due to the Z-shaped monopole of length d_{t1} ($d_S+d_2+d_3+d_4+d_5+d_6$). However, it is observed that the current through the C-shaped path

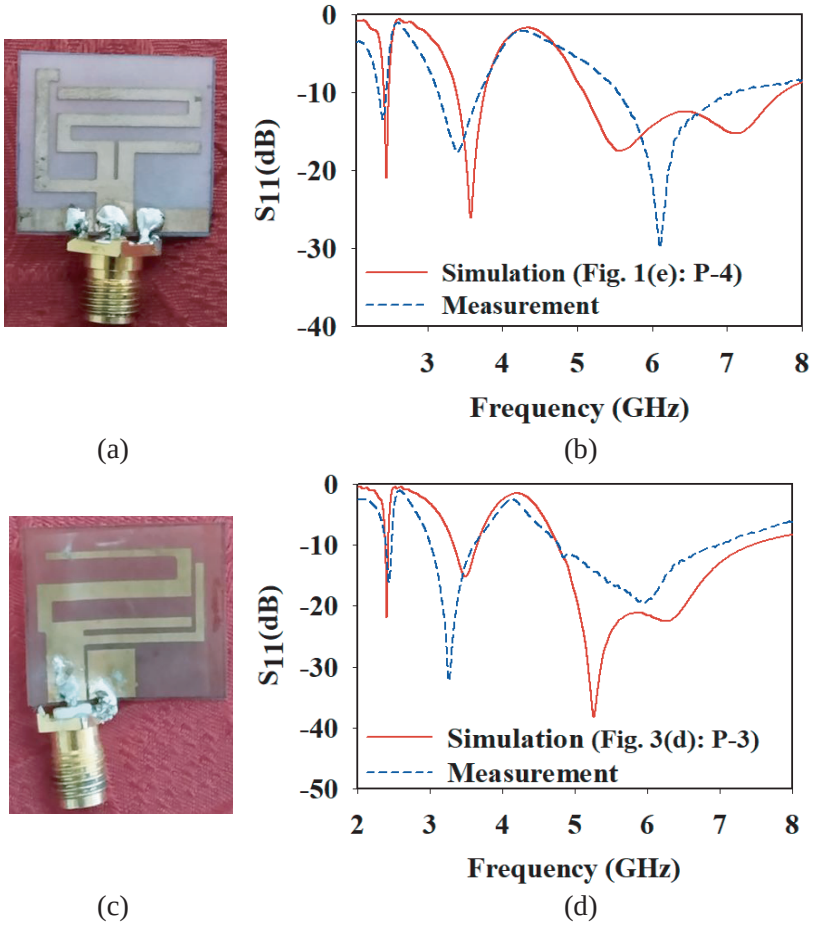

Figure 5. (a) Prototype of CPW-fed TBFMA (b) reflection coefficient plot of CPW-fed TBFMA (c) prototype of ACS-fed TBFMA (d) reflection coefficient plot of ACS-fed TBFMA.

length $d_{t2}(d_m + d_7 + d_8 + d_9)$ also contributes to this. The effective resonance length (d_{t1}) at 2.45 GHz is $0.47\lambda_{d1}$, and d_{t2} is $0.24\lambda_{d1}$, where λ_{d1} is the effective wavelength at f_1, calculated as follows [15, 16];

$$\lambda_d = \frac{c}{f\sqrt{\varepsilon_{efft \cdot r}}} \tag{11}$$

$$\varepsilon_{efft \cdot r} = \varepsilon_{efft} - \frac{\varepsilon_{efft} - 1}{\frac{(m-n)/2}{0.7r} \cdot \frac{K(k)}{K'(k)} + 1} \tag{12}$$

$$\varepsilon_{efft} = 1 + \frac{\varepsilon_r - 1}{2} \cdot \frac{K(k')K(k_p)}{K(k)K(k'_p)} \tag{13}$$

$$k_p = \frac{\sinh\left(\frac{\pi n_r}{4h}\right)}{\sinh\left(\frac{\pi m_r}{4h}\right)} \tag{14}$$

$$n_r = n + \frac{1.25r}{\pi}\left[1 + \ln\left(\frac{4\pi n}{r}\right)\right] \tag{15}$$

$$m_r = m - \frac{1.25r}{\pi}\left[1 + \ln\left(\frac{4\pi n}{r}\right)\right] \tag{16}$$

where n is the feed width, r the conductor thickness, ε_{efft} the effective dielectric constant, $m = n + 2g_p$

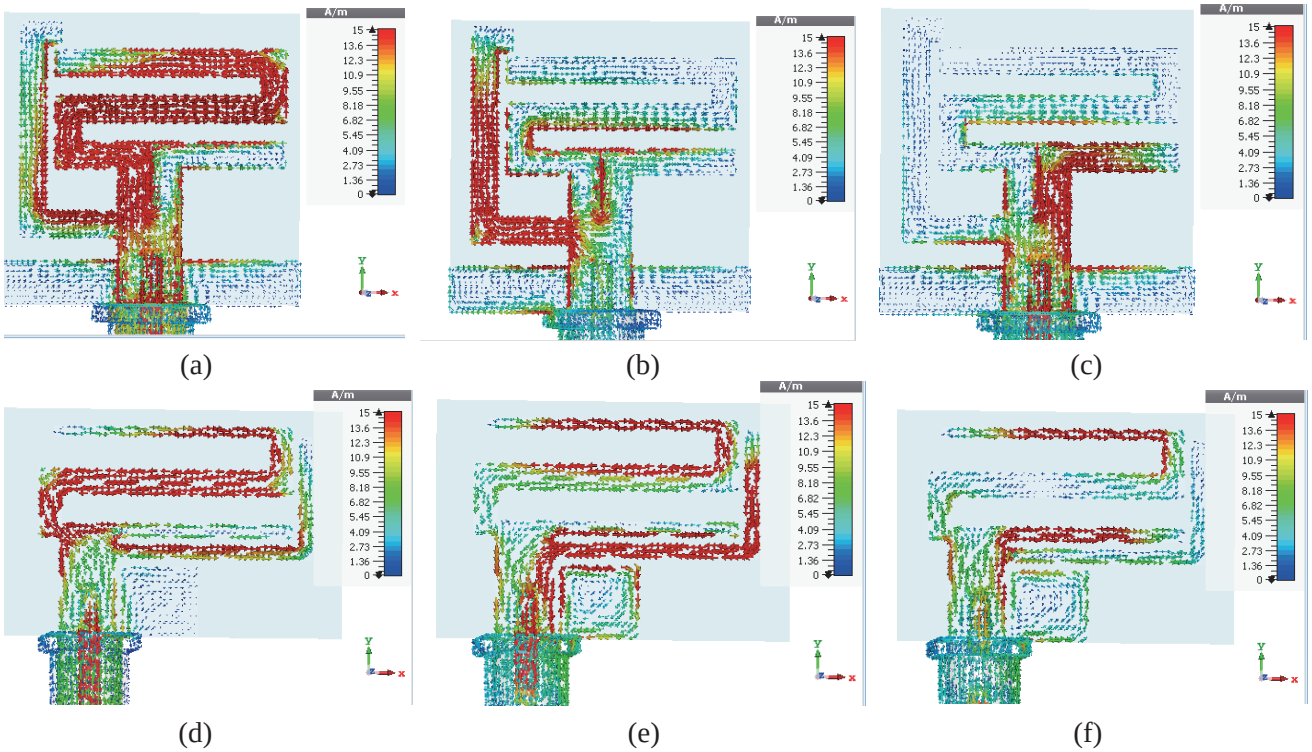

Figure 6. Surface current plots of the CPW-fed TBFMA at (a) 2.45 GHz, (b) 3.57 GHz, (c) 5.5 GHz, and the ACS-fed TBFMA at (d) 2.4 GHz, (e) 3.5 GHz, (f) 5.3 GHz.

and $k = \frac{n}{m}$.

As seen in Fig. 6(b), the resonance at 3.57 GHz is due to the current path d_m, d_7, d_8, and d_9 in the C-shaped strip. The effective resonance length (d_{t2}) is $0.35\lambda_{d2}$. The inverted L strip makes up most of the contribution at 5.5 GHz. The current path d_s and d_1 is shown in Fig. 6(c), and corresponding length (d_{t3}) is $0.29\lambda_{d3}$.

Figures 6(d)–(f) show the surface current plots of ACS-fed TBFMA at 2.4 GHz, 3.5 GHz, and 5.3 GHz. The resonance at 2.4 GHz shown in Fig. 6(d) is mainly due to the Z-shaped monopole of length d_{t1} ($d_S + d_2 + d_3 + d_4 + d_5 + d_6$). However, it is observed that the current through the L-shaped path length d_{t2} ($d_m + d_7 + d_8$) also contributes to this. The effective resonance length (d_{t1}) at 2.4 GHz is $0.407\lambda_{d1}$, and d_{t2} is $0.2\lambda_{d1}$, where λ_{d1} is the effective wavelength at f_1, calculated as follows [15, 16];

$$\lambda_d = \frac{c}{f\sqrt{\varepsilon_{efft}}} \tag{17}$$

$$\varepsilon_{efft} = 1 + t(\varepsilon_r - 1) \tag{18}$$

$$t = \frac{K(k_r)}{K'(k_r)} \frac{K'(k_q)}{K(k_q)} \tag{19}$$

$$k_r = \sqrt{\frac{\sinh(\pi n/2h)e^{-\pi g_p/2h}}{\sinh(\pi(n+g_p)/2h)}} \tag{20}$$

$$k_q = \sqrt{\frac{n}{n+g_p}} \tag{21}$$

where n is the feed width, and ε_{efft} is the effective dielectric constant. As seen in Fig. 6(e), the resonance at 3.5 GHz is due to the current path d_m, d_7, and d_8 in the L-shaped strip. The effective resonance length (d_{t2}) is $0.296\lambda_{d2}$. The inverted L strip d_s and d_1 makes up most of the contribution at 5.3 GHz. The current path is shown in Fig. 6(f), and corresponding length (d_{t3}) is $0.28\lambda_{d3}$.

The measured E (YZ) and H (XZ) plane 2D patterns of the proposed CPW-fed TBFMA and ACS-fed TBFMAs are shown in Figs. 7(a)–(c) and 7(d)–(f). The 3D patterns of the proposed CPW-fed and ACS-fed TBFMAs shown in Fig. 8 were measured using EMSCAN — RFXpert. Measured average gains of the proposed CPW-fed TBFMA in lower, middle, and upper frequency bands are 0.5 dBi, 1.1 dBi, and 2.5 dBi. The corresponding average gains of the ACS-fed TBFMA are 0.9 dBi, 1.8 dBi, and 5 dBi.

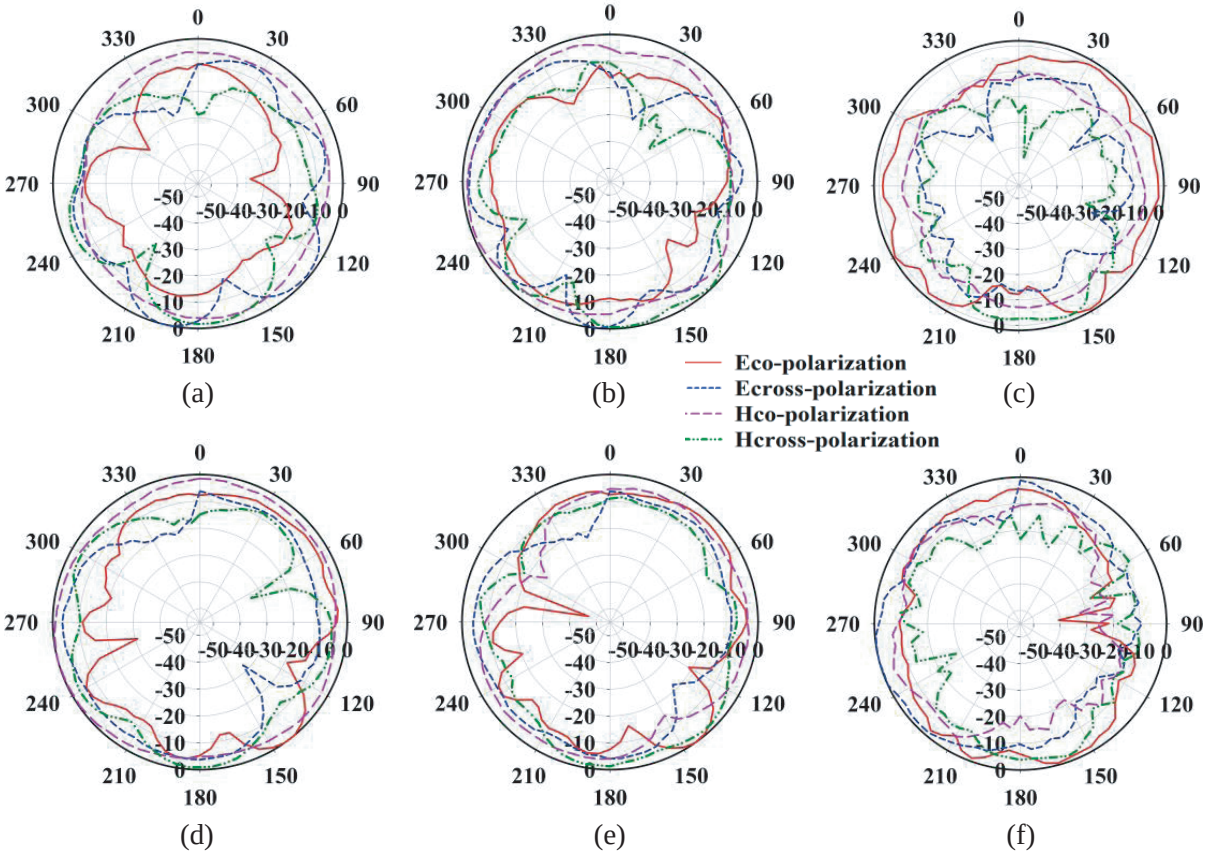

Figure 7. Measured E (YZ) and H (XZ) plane 2D patterns of the CPW-fed TBFMA at (a) 2.45 GHz, (b) 3.5 GHz, (c) 5.5 GHz, and the ACS-fed TBFMA at (d) 2.4 GHz, (e) 3.5 GHz, (f) 5.3 GHz.

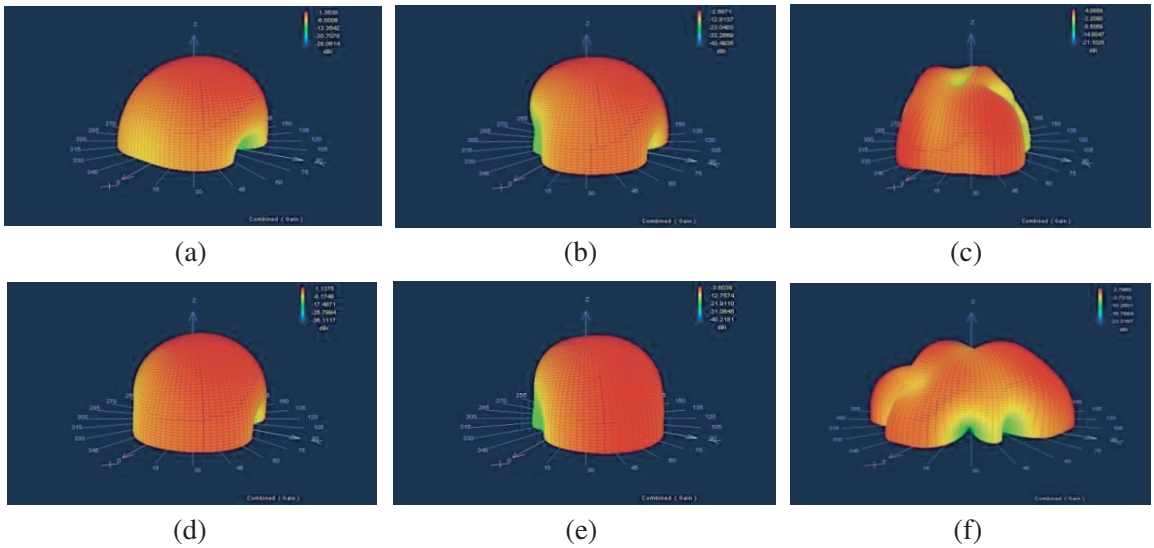

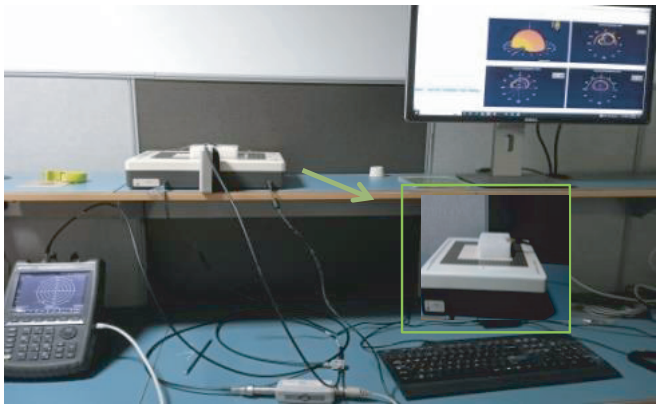

(g)

Figure 8. Measured 3D patterns of the CPW-fed TBFMA in XZ plane at (a) 2.45 GHz, (b) 3.5 GHz, (c) 5.5 GHz, and the ACS-fed TBFMA in XZ plane at (d) 2.4 GHz, (e) 3.5 GHz, (f) 5.3 GHz, (g) 3D pattern measurement set up.

4. FLEXIBILITY STUDIES

The flexibility of the substrate permits the TBFMA to be incorporated into numerous smart devices in a bent condition. The performance of the proposed antennas is investigated in various bending scenarios by bending the TBFMA on air cylindrical tubes with different radii. Figs. 9(a)–(b) show the simulated S_{11} (dB) of the CPW-fed TBFMA (XZ plane) under inward and outward bending on different radii cylinders. Figs. 9(c)–(d) show the simulated S_{11} (dB) of the ACS-fed TBFMA (XZ plane) under inward and outward bending on different radii cylinders. The results demonstrate that the ACS-fed TBFMA is less susceptible to bending than the CPW-fed TBFMA, as a result of its uniplanar nature

Table 3. Comparison of various multi-band antennas.

Ref./year	**Dielectric**	**Operating Bands (GHz)**	**Overall dimension (mm^2)**	**Flexibility**
[1]/2020	ROGERS RO4835T ($\varepsilon_r = 3.52$, $\tan\delta = 0.003$)	2.35–2.5/3.18–3.82/4.15–5.42	25×32	Yes
[2]/2020	Flexible Polyamide ($\varepsilon_r = 4.3$, $\tan\delta = 0.004$)	2.33–2.47/3.68–3.92/5.38–5.75	24×19	Yes
[3]/2021	Polyimide film ($\varepsilon_r = 3.5$, $\tan\delta = 0.004$)	2.28–2.51/5.2–6/5–4	30×30	Yes
[5]/2021	Fr4 ($\varepsilon_r = 4.4$, $\tan\delta = 0.02$)	1.96–2.22/3.51–3.91/4.78–5.26	37×28	No
[4]/2022	Fr4 ($\varepsilon_r = 4.4$, $\tan\delta = 0.02$)	2.37–2.51/3.34–3.71/4.6–6.4	20×15	No
Proposed TBFMA				
CPW fed	**Dupont (ε_r= 3.5, tanδ =0.027)**	**2.35–2.48/3.1–3.7/5.5–7.05**	**19×19**	**Yes**
ACS fed	**Dupont (ε_r= 3.5, tanδ =0.027)**	**2.39–2.47/3–3.6/4.78–7**	**19.5×15**	**Yes**

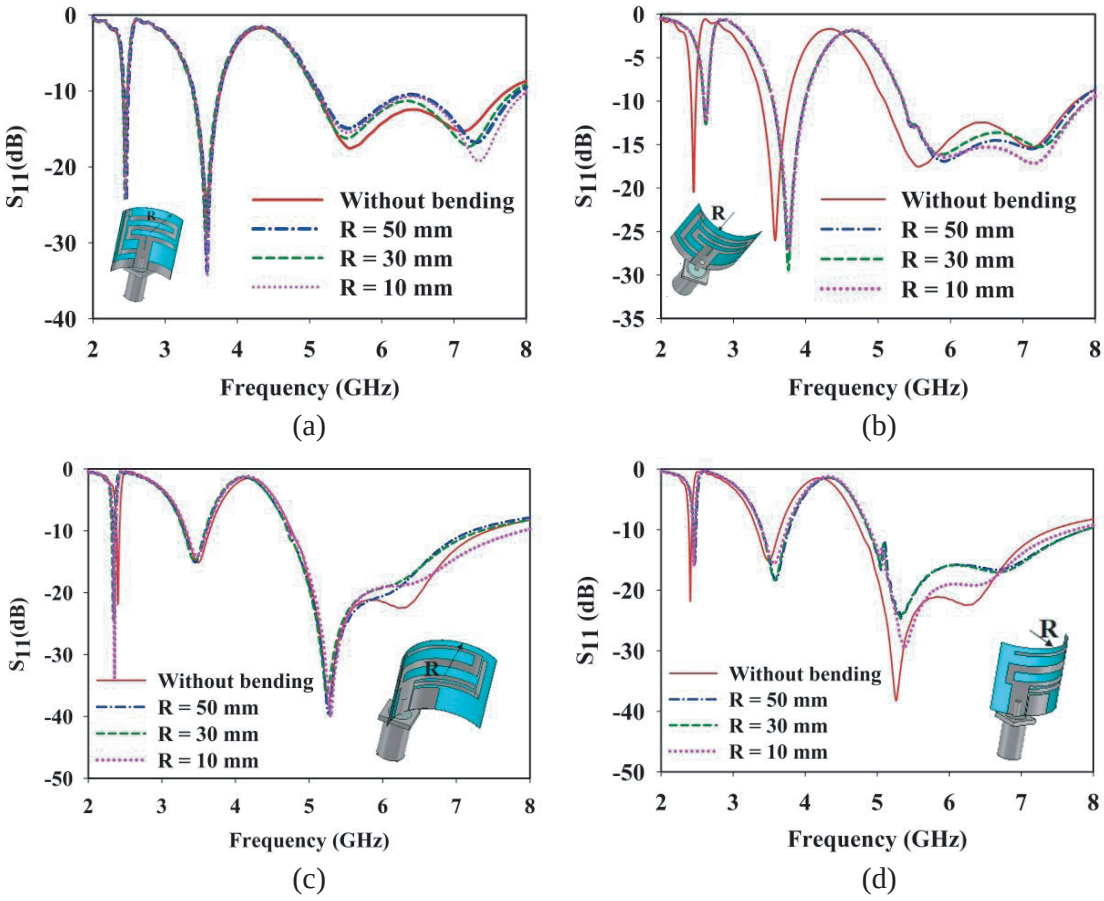

Figure 9. Flexibility studies: simulated S_{11} (dB) of the CPW fed TBFMA (XZ plane) under (a) inward bending, (b) outward bending, and the ACS fed TBFMA under (c) inward bending, (d) outward bending.

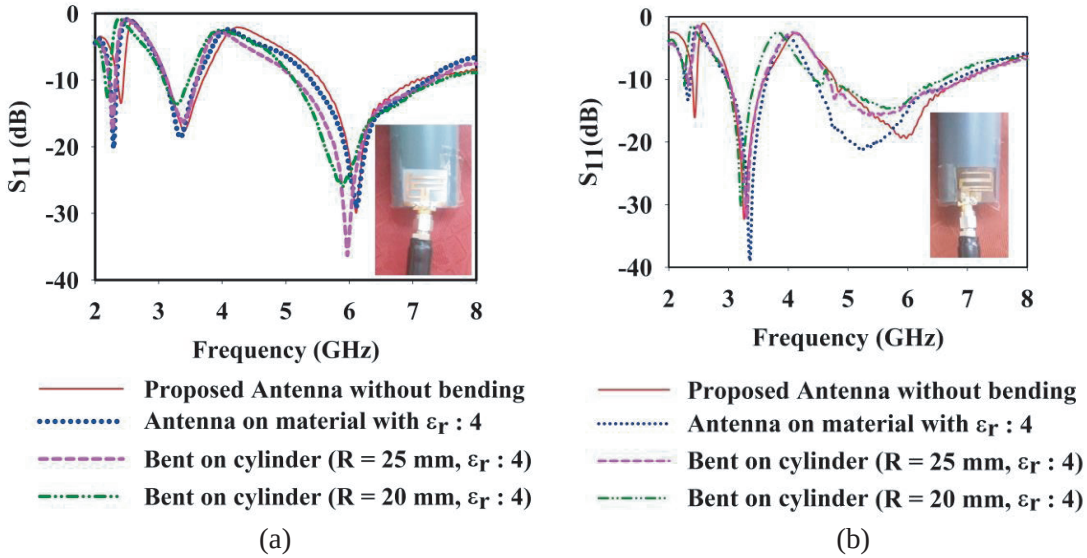

Figure 10. Flexibility studies: measured S_{11} (dB) of the TBFMA bending on cylindrical tubes (radius: R and ε_r : 4). (a) CPW fed TBFMA. (b) ACS fed TBFMA.

and asymmetrical design. Fig. 10 shows the measured S_{11} (dB) plot of the proposed TBFMA bending on cylindrical tubes with radius R and dielectric constant (ε_r) : 4. The findings prove that the antennas retain their tri-band characteristics regardless of the radius of the bend.

Table 3 compares the proposed TBFMA with existing multi-band antennas. The compactness of the proposed antennas is evident from the table.

5. CONCLUSION

The tri-band flexible monopole antennas with coplanar waveguide (CPW) feed and asymmetric coplanar strip (ACS) feed presented in this paper are ultra compact. The extremely thin Dupont material (ε_r : 3.5 and $\tan\delta$: 0.027) used as the substrate makes the antenna flexible. A simple geometry with folded structure enables easy fabrication of the antenna. The CPW-fed antenna (19 mm × 19 mm) exhibits bandwidths of 130 MHz, 600 MHz, and 1550 MHz in the lower, middle, and upper frequency bands. The ACS-fed antenna (19.5 mm × 15 mm) exhibits bandwidths of 80 MHz, 600 MHz, and 2220 MHz in the lower, middle, and upper frequency bands, catering to ISM 2.4/5.2 GHz, Wi-Fi 2.4/5 GHz, WLAN 2.4/5.2/5.8 GHz, and WiMAX 3.5/5.5 GHz. The circuit model and design equations presented in this paper give a good theoretical support for the performance evaluation of these proposed antennas. The antennas are found to maintain their performance under different bending conditions. Simple geometry, compactness, excellent flexibility, and stability under bending conditions over multiband make these extremely thin antennas quite attractive.

REFERENCES

1. Zaidi, A., W. A. Awan, N. Hussain, and A. Baghdad, "A wide and tri-band flexible antennas with independently controllable notch bands for sub-6-GHz communication system," *Radioengineering*, Vol. 29, 44–51, 2020.
2. Sreelakshmi, K., G. S. Rao, and M. N. V. S. S. Kumar, "Compact GACS-fed flexible multiband reconfigurable antenna for wireless applications," *IEEE ACCESS*, Vol. 8, 194497–194507, 2020.
3. Lai, J., J. Wang, W. Sun, R. Zhao, and H. Zeng, "A low profile artificial magnetic conductor based tri-band antenna for wearable applications," *Microw. Opt. Technol. Lett.*, 1–7, 2021.
4. Hussain, N., A. Abbas, S. M. Park, S. G. Park, and N. Kim, "A compact tri-band antenna based on inverted-L stubs for smart devices," *Computers Materials & Continua, CMC*, Vol. 70, 3321–3331, 2022.
5. Nallapaneni, S. and P. Muthusamy, "Design of multiband fractal antenna loaded with parasitic elements for gain enhancement," *Int. J. RF Microw. Comput. Aided Eng.*, Vol. 31, 1–8, 2021.
6. Chu, H. B. and H. Shirai, "A compact metamaterial quad-band antenna based on asymmetric E-CRLH unit cells," *Progress In Electromagnetics Research C*, Vol. 81, 171–179, 2018.
7. Liu, H., P. Wen, S. Zhu, B. Ren, X. Guan, and H. Yu, "Quad-band CPW-fed monopole antenna based on flexible pentangle-loop radiator," *IEEE Antennas and Wireless Propagation Letters*, Vol. 14, 1373–1376, 2015.
8. Anil Kumar, C. V., B. Paul, and P. Mohanan, "Compact triband dual F-shaped antenna for DCS/WiMAX/WLAN applications," *Progress In Electromagnetics Research Letters*, Vol. 78, 97–104, 2018.
9. Ahmad, H., W. Zaman, S. Bashir, and M. U. Rahman, "Compact triband slotted printed monopole antenna for WLAN and WiMAX applications," *Int. J. RF Microw. Comput. Aided Eng.*, 1–8, 2019.
10. Lakshmanan, R., S. Mridul, A. Pradeep, P. Mohanan, and R. Moolat, "Compact ACS-fed flexible monopole antenna for dual band applications," *International Journal of Microwave and Optical Technology*, Vol. 17, 355–365, 2022.
11. Lakshmanan, R., S. Mridula, and P. Mohanan, "Compact dual-band flexible antenna for WLAN/Wi-Fi applications," *IEEE International Symposium on Antennas and Propagation and USNC/URSI National Radio Science Meeting*, 451–452, Boston, MA, USA, 2018.

12. Vashi, R. and T. Upadhyaya, "CPW fed flexible graphene based thin dual band antenna for smart wireless devices," *Progress In Electromagnetics Research M*, Vol. 89, 73–82, 2020.
13. Mohammed, M., B. Suwailam, and A. Alomainy, "Flexible analytical curve-based dual-band antenna for wireless body area networks", *Progress In Electromagnetics Research M*, Vol. 84, 73–84, 2019.
14. Ghaffar, A., W. A. Awan, N. Hussain, S. Ahmad, and X. J. Li, "A compact dual-band flexible antenna for applications at 900 and 2450 MHz," *Progress In Electromagnetics Research Letters*, Vol. 99, 83–91, 2021.
15. Garg, R., P. Bhartia, and I. Bahl, *Microstrip Antenna Design Hand book*, 1st Edition, Artech House, MA, 2001.
16. Simons, R. N., *Coplanar Waveguide Circuits, Components, and Systems*, John Wiley & Sons, Inc., 2001.